International Journal of Modern Physics C

Influence of the disorder correlation length on localization and quantum state transference in tight-binding channels

J. D. S. Silva[1,2], G. M. A. Almeida[1], M. L. Lyra[1], F. A. B. F. de Moura[1]

1) Instituto de Física, Universidade Federal de Alagoas, Maceió, AL, 57072-970, Brazil //
2)Centro de Informática, Universidade Federal de Pernambuco, Recife, PE, 50740-560, Brazil

Received Day Month Year
Revised Day Month Year

We investigate in detail the transference of quantum states in a disordered channel. We consider a one-dimensional tight-binding model consisting of a source S connected to a receiver R throughout a disordered channel. The disorder distribution contains a single tunable spatial correlation length. We demonstrate that the disorder correlation length plays a relevant role within the localization properties of the channel. The hopping parameter between the sites S and R and the channel are also adjustable parameters. We investigate the possibility of transference of quantum states along this quantum channel model and describe the optimal conditions for the occurrence of a high fidelity process.

Keywords: tight-binding model, correlated disorder, localization

PACS Nos.:

1. Introduction

In recent years, theoretical and experimental research on quantum information processing have become a very active field in physics.[1–9] Among the many challenges to be addressed in order to make quantum devices more practical, there is the development of robust quantum-state transfer (QST) protocols between processing units.[10–12] Most of the existing communication protocols are based on photons due to their weak interaction with the environment and groundbreak achievements in fiber technology. On the other hand, when dealing with quantum devices it is not always feasible to convert photons back and forth to stationary qubits.[13]

One of the ways to implement QST with minimum degree of control is by engineering the quantum channel and dynamics beforehand on stationary qubits. The goal is to prepare an arbitrary quantum state at one location and see whether the natural temporal evolution of the system is capable of bringing it to another location with good fidelity. A burst of QST schemes came forth after S. Bose proposed the use of spin-1/2 chains as channels for short-distance communication.[14] One solution is to design the couplings of the spin chain so that quantum-state transfer as well as generation of entanglement become size-independent.[14,15] This can be done upon considering long-range interactions. The idea is to create an optimiza-

tion scheme to approximate the ideal behavior, which keeps the interaction strength reasonably high while the sender and receiver are effectively detached from the rest of the chain.[13,16] Such a procedure is scalable with the size of the system as the authors showed that both QST fidelity time becomes invariant and approach ideal values.[13,16]

Recently, a single-qubit QST protocol was addressed on an anisotropic Heisenberg XXZ model in 1D, 2D, and 3D networks, where the couplings followed a power law with a variable exponent.[12] For regular networks, it is verified that the fidelity increases with the dimensionality of the network for sufficiently large systems and this becomes more evident in the case of 1D networks featuring long-range interaction. In addition, it has been shown that such class of systems are more robust against temperature-induced disorder than those having short-range interactions.[12]

A high degree of resilience against disorder has also been reported in a QST protocol defined on a Su-Schrieffer-Heeger (SSH) chain.[17] This scheme combines an immediate change in the state of the topological border with fine tuning of interactions between nearest neighbors. It is shown that the presence of spatial correlations in the disorder distribution aids to the robustness of the protocol.[17] In general, the role of disorder in QST protocols is something that cannot be ignored and has been extensively investigated in recent years.[18–20] An immediate result is that most of the QST protocols are robust to uncorrelated disorder to some extent, specially those involving weak links between the sender/receiver and the channel.[21] However, things get more involved in the presence of correlated disorder, when its degree of correlation can actually improve the QST performance.[19]

In this work we consider a disordered one-dimensional model featuring tunable spatial correlations working as the communication channel between two parties S and R. We seek to optimize their communication in the presence of such disorder by adjusting the coupling strength between the channel and them. The paper is organized as follows. In section 2, we introduce the Hamiltonian of the model, show how to generate the correlated disorder potential and introduce the main quantities we are going to use to analyze the localization and quantum state transfer process. Section 3 contains our numerical results together with a detailed discussion of the role played by the disorder correlation length on the localization and QST process. A summary and conclusions is offered in Sec. 4.

2. Model and Methodology

In the following, we will consider a channel model that consists of a one-dimensional chain of atoms, built from a source, $|S\rangle$, a main channel C with L atoms, and a receiver $|R\rangle$. The full model contains $L+2$ atoms. The Hamiltonian is given by:

$$\hat{H} = |S\rangle\langle S|\,\varepsilon_S + g(|S\rangle\langle 2| + |L+1\rangle\langle R|) + |R\rangle\langle R|\,\varepsilon_R + \hat{H}_c, \tag{1}$$

where g is the hopping amplitude between the atoms $|s\rangle$ and $|2\rangle$ and between $|L+1\rangle$ and $|R\rangle$. ε_S and ε_R are the on-site potentials on the source (S) and the receiver

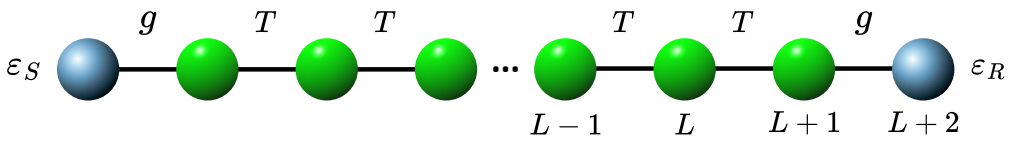

Fig. 1. Communication channel between Sender and Receiver sites. The channel is composed of L sites with random on-site potentials with a typical disorder correlation length.

(R). The channel Hamiltonian $\hat{H}_c$ is given by:

$$\hat{H}_c = \sum_{i=2}^{L+1} \varepsilon_i \left|i\right\rangle \left\langle i\right| + T \sum_{i=2}^{L+1} (\left|i+1\right\rangle \left\langle i\right| + h.c), \tag{2}$$

where $T = 1$ is the hopping amplitude between the atoms within the chain. The set $\{\varepsilon_i\}$ is a series with correlated disorder generated following the procedure below. Initially, we consider the correlated sequence defined as:

$$y_i = \sum_{j=1}^{L} z_j / (1 + |i-j|/A)^2, \tag{3}$$

where z_j is a random number belonging to the range $[-1, 1]$, and A is an adjustable parameter that controls the correlation degree within the sequence of number $\{y_i\}$. Therefore, the on-site disorder distribution ε_i is constructed as follows:

$$\varepsilon_i = (y_i - \langle y_i \rangle) / \sqrt{\langle y_i^2 \rangle - \langle y_i \rangle^2}. \tag{4}$$

It is important to note that the procedure we are discussing is applicable only when the value of A/L is finite. Our focus is on channels with correlated disorder. The situation where $A/L \to \infty$ is a limit that does not involve any disorder. Therefore, we will not consider this scenario. The auto-correlation of the set $\{\varepsilon_i\}$ can be obtained by:

$$C(r) = \langle \varepsilon_i \varepsilon_{i+r} \rangle - \langle \varepsilon_i \rangle \langle \varepsilon_{i+r} \rangle , \tag{5}$$

where $\langle \varepsilon_i \varepsilon_{i+r} \rangle$ is given by:

$$\langle \varepsilon_i \varepsilon_{i+r} \rangle = \frac{1}{L-r} \sum_{i=1}^{L-r} \varepsilon_i \varepsilon_{i+r}$$

$$\langle \varepsilon_i \rangle = \sum_{i=1}^{L} \varepsilon_i / L$$

Figure 2 shows a graphical representation of the auto-correlation function versus the distance, calculated for several values of A. Notice that the auto-correlation function decreases rapidly with distance for small values of A. For larger values of A, the correlation function exhibits a slower decay. In all cases, the auto-correlation function decays exponentially, a characteristic of disordered correlated systems with

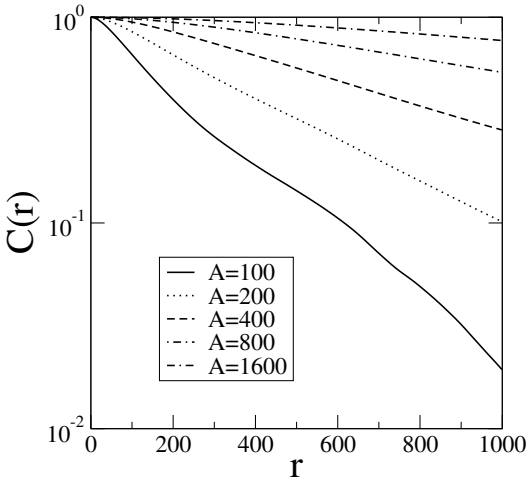

Fig. 2. Auto-correlation function of the on-site potentials series for different values of A. The typical exponential decay length is proportional to the disorder control parameter A.

a typical correlation length. In the present model, the adjustable parameter A acts as this typical length scale of the disorder distribution. The diagonalization of the Hamiltonian provides the eigenstates $|\Psi_i\rangle$ and the eigenvalues E_i. We can expand the eigenstates on the orbital basis ($|\Psi_i\rangle = \sum_{n=1}^{L} f_n^i \, |n\rangle$). Participation ($P$) is a number that measures the degree of the localization of all eigenstates. For the $i-th$ eigenstate the participation is given by:[22–24]

$$P^i = \frac{1}{\sum\limits_n |f_n^i|^4} \tag{6}$$

We emphasize that the participation number represents the typical number of sites on which the quantum state is effectively distributed. For localized states, the participation number remains finite (roughly independent of L). For extended states, the participation number is proportional to L^1 (considering the topological dimension $d = 1$). Another measure to obtain the degree of localization of the system is the Shannon entropy, which is given by:[25]

$$S^i = -\sum_n |f_n^i|^2 log(|f_n^i|)^2 \tag{7}$$

At the logarithm scale, the Shannon entropy exhibits a finite-size scaling similar to those obtained for the participation number. For extended states, S is proportional to $\log(L)$ while S is roughly a constant for localized ones.

We also analyzed the transference of quantum states along this quantum channel model. The procedure consists of solving the time-dependent Schrödinger equation to obtain the time-dependent wave-function at the site $L + 2$. To obtain the time-dependent wave-function $|\phi(t)\rangle = \sum_n X_n(t) \, |n\rangle$ we used the evolution operator

procedure $|\phi(t)\rangle = e^{-i\mathcal{H}t}\,|\phi(t=0)\rangle$. By applying the evolution operator,[26] we obtain the time-dependent wave-function components $X_n(t)$ as:

$$X_n(t) = \sum_j \{A_j f_n^j e^{-iE_j t}\} \tag{8}$$

where $A_j = \sum_l X_l(t=0) f_l^j$. To investigate the transfer of quantum states, we calculate the concurrence and Fidelity. The concurrence[27] between the source S and receiver R is expressed as

$$C(t) = 2|X_1(t)X_{L+2}(t)|, \tag{9}$$

which goes from 0 (no entanglement) to 1 (maximum entanglement). The Fidelity function is defined as[20]

$$F(t) = \frac{1}{2} + \frac{|X_{L+2}(t)|}{3} + \frac{|X_{L+2}(t)|^2}{6}, \tag{10}$$

which measures how the quantum state at the Receiver is similar to the initial state at the Sender. It becomes unity when state at the receiver reproduces the initial state at the Sender, approaching 1/2 in the absence of fidelity. In the following, we will focus on the maximum concurrence $C_{max} = \max[C(t)]$ and the maximum fidelity $F_{\max} = \max[F(t)]$ conditions. In our calculations, we have used a time interval $t > 6 \times 10^5$ and about 1000 distinct disorder realizations to compute C_{max} and $F_{\max}$. Whenever the transference of quantum states occurs with good efficiency, the functions C_{max} and $F_{\max}$ become close to unity. However, if quantum state transference does not succeed, $C_{max} \approx 0$ and $F_{\max} \approx 0.5$.

3. Results

We start our analysis by showing a detailed study of the localization aspects of eigenstates in the presently considered correlated disordered channel. We perform an exact diagonalization of the complete Hamiltonian for several values of L and A. *We have performed the complete diagonalization using a Lapack routine called $SSTEDC$[28] in Fortran. Additionally, we have employed another Lapack routine called $SSTEGR$[28] to diagonalize around the band center partially. This last routine enables considering large system sizes in less computational time.* In figure 3 we present the participation versus energy for different A values. When A assumes small values, the participation has almost no dependency on L. However, as A becomes larger, we notice that, around the band center, exists a more evident dependency with L (see, for example, the curves for $A = 80$ and $A = 160$). To explicitly evaluate the role played by the correlation length A, we study the behavior of the maximum participation, in the center of the band, for several chain sizes and correlation lengths A, as seen in figure 4(a). Our calculations averaged the participation number using more than 200 distinct disorder samples. Therefore, the average participation number is given by $P_{max} = \sum_{|E_j|<\Delta E} P^j/N_E$ with $\Delta E = 0.05$ and N_E the number of states with energy between $-\Delta E$ and ΔE. Calculations were done

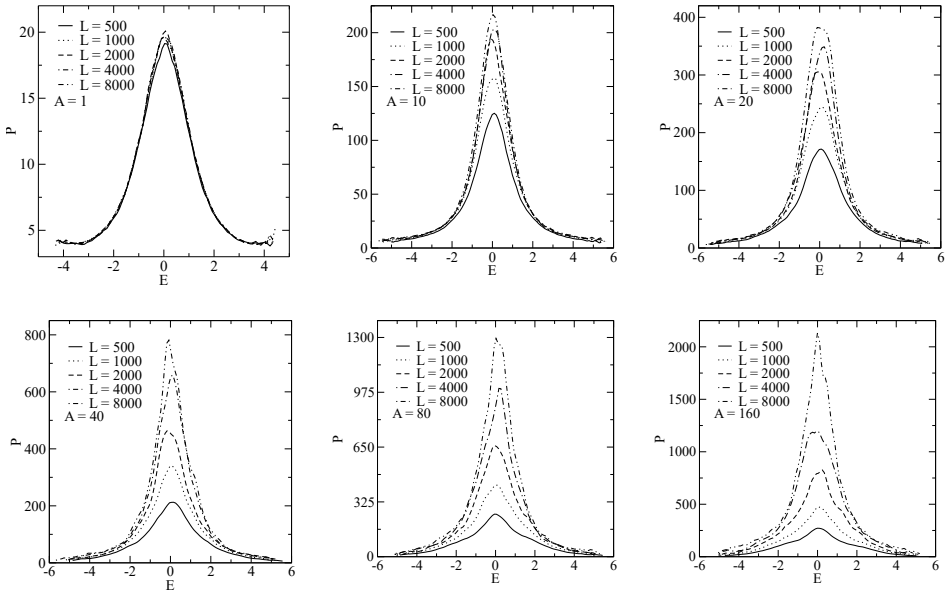

Fig. 3. The participation number versus E for $L = 500$ up to 8000 and several values of A. For large A values, the participation length scales with the chain size, a typical behavior of channels presenting effectively delocalized eigenstates.

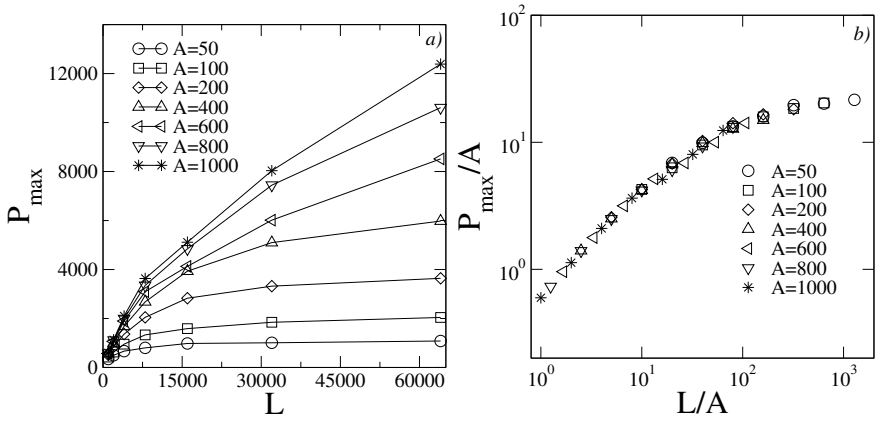

Fig. 4. a) Maximum participation number (P_{max}) versus L for $A = 50$ up to 1000. b) Data collapse of all curves of (a) using a universal scaling function $P_{max}/A = f(L/A)$. The initial linear growth accounts for the regime of effectively delocalized states. The saturation represents the ultimate Anderson localization regime.

using $L = 1000$ up to 64000. and $A = 50$ up to 1000. Our results indicate that, independent of the value of A considered here, the size dependence of the participation

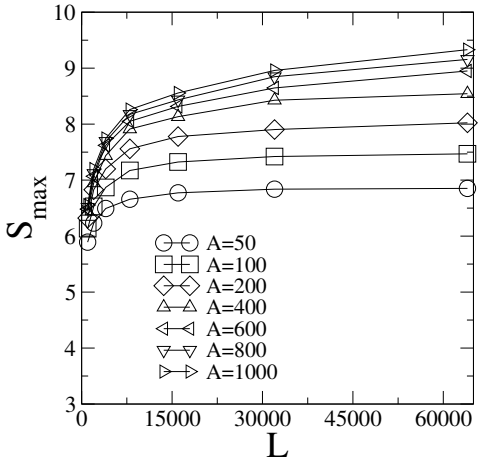

Fig. 5. Shannon entropy versus L for $L = 1000$ up to 64000 and $A = 50$ up to 1000. The main trends are in good agreement with the results obtained for the participation number.

number suggest Anderson localization. We can observe that P_{max}, even for large A, is weakly dependent on L. To extract the universal character, we proceed with a finite-size scaling analysis. We re-scale both axis (P_{max} and L) by the value of A. Using this re-scaled variables (P_{max}/A and L/A) we collapse all curves in a unique universal curve (see fig.4(b)). Therefore the re-scaled participation number P_{max}/A exhibits a typical behavior : $P_{max}/A = f(L/A)$. The single branch within the data collapse confirms the localized nature of the eigenstates. For $L/A >> 1$ (the regime of short correlation length $A << L$), the participation becomes independent of the system size, a typical behavior of localized states. Further, it becomes proportional to the disorder correlation length A. On the opposite regime of $L/A << 1$ (long correlation length $A >> L$), the participation becomes independent of A, scaling proportionally to the channel size L, a characteristic of effectively extended states.

In fig. 5 we plot our results for the Shannon entropy (S) versus L considering L from 1000 up to 64000 and $A = 50$ up to 1000. The main results are qualitatively similar to those obtained using the participation number. Even for large A, the Shannon entropy seems almost independent of L (in the limit of large $L >> A$). Based on this analysis, we can conclude that this model does not contain truly extended states in the thermodynamic limit. However, the effective localization length of eigenstates around the band center increases until it reaches values of the same order as the system size for large A. This regime favors the possibility of transferring the quantum state from the Sender to the Receiver site.

Let us investigate investigate the transference of quantum states around $\varepsilon = 0$ in more detail. We initially present some results for the normalized probability densities $P(F_{max})$ and $P(C_{max})$. We emphasize that we calculate both quantities $F_{max} = max(F(t))$ and $C_{max} = max(C(t))$ for times up to 6×10^5 for over 1000 distinct disordered samples. We also emphasize that in our first numerical experiment, the

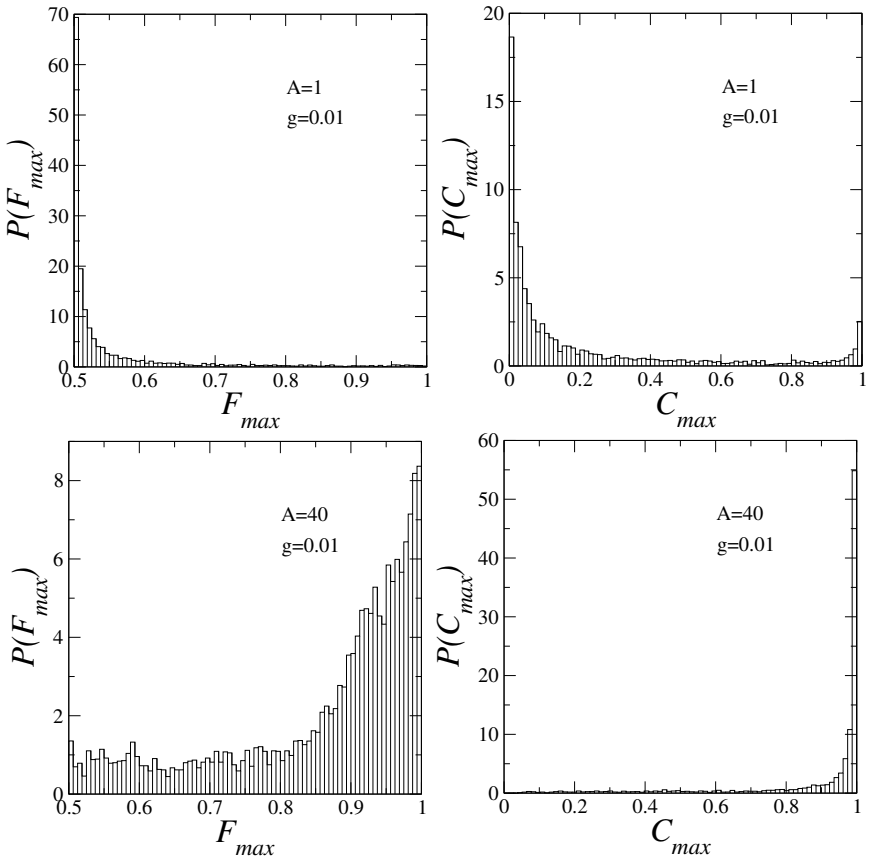

Fig. 6. Normalized probability distributions $P(F_{max})$ and $P(C_{max})$ for $A = 1, 40$ and $g = 0.01$. Calculations of $F_{max} = max(F(t))$ and $C_{max} = max(C(t))$ were done using time runs up to 6×10^5 and over 1000 distinct disorder realization.

on-site energy of the source (S) and the receiver (R) was chosen as $\epsilon_S = \epsilon_R = \epsilon = 0$. From ($F_{max}$) and ($C_{max}$) reached for each sample, we calculate the normalized distribution $P(F_{max})$ and $P(C_{max})$ shown in fig .6 for $A = 1$ and $A = 40$. For $A = 1$, the probability distribution suggests that the most frequent values of F_{max} and C_{max} are roughly about 0.5 and 0. These results indicate the absence of quantum transference from S up to R. For $A = 40$, our calculations indicate that an efficient transference along the channel is possible. The probability distribution indicates that $F_{max} \approx 1$ and $C_{max} \approx 1$ are frequently obtained in our numerical experiments.

We also investigate the dependence of (F_{max}) and (C_{max}) on the on-site energy in the Sender and Receiver sites $\epsilon_S = \epsilon_R = \epsilon$. In figure 7 on the left, we have the representation of the average maximum fidelity versus ϵ. We calculate the fidelity for various values of A. When $A = 1$, the fidelity is approximately 0.5, and the system does not show a reliable QST. However, for higher values of A, the fidelity approaches 0.9 around $\epsilon = 0$ (the average on-site potential along the channel), offer-

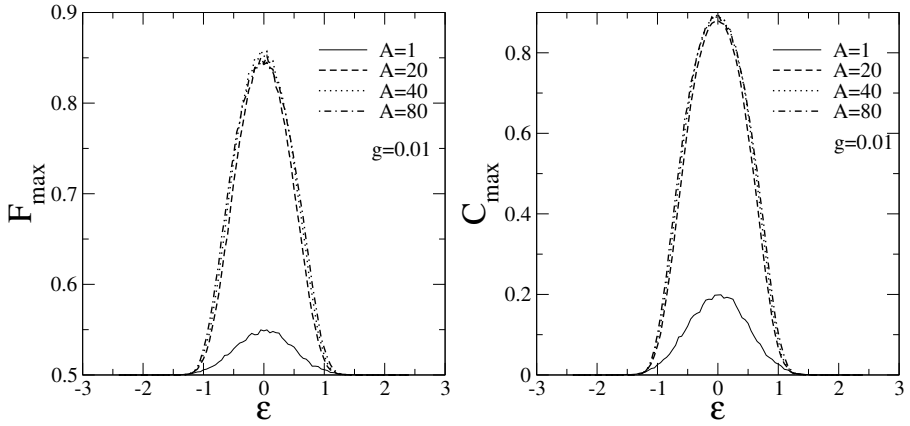

Fig. 7. Maximum Fidelity (left) and Concurrence (right) versus the Sender and Receiver on-site potential $\varepsilon_S = \varepsilon_R = \varepsilon$ for $L = 60$, $g = 0.01$, and $A = 1$ up to 80. We observe that both quantities indicate the absence of quantum transference for $A = 1$. For large A, one reaches an effective quantum state transference with good fidelity.

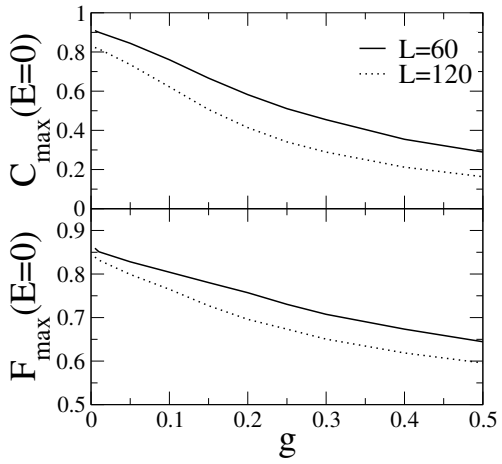

Fig. 8. Maximum Fidelity and Concurrence for $\varepsilon = 0$ versus the strength g of the coupling between the sender and receiver sites with the communication channel, for $A = 40$, $L = 60$ and 120. For $g << 1$, both quantities (F_{max} and C_{max}) approach unit, thus indicating the existence of efficient quantum state transference. For $g \approx 1$ no effective quantum transference can be realized.

ing a good QST. This same result can be seen in the concurrence versus ϵ depicted in figure 7 on the right. For $A = 1$ we have the concurrence of approximately 0.2, showing that the system does not present enough entanglement between S and R. For higher values of A the entanglement grows, approaching maximum entanglement around $\epsilon = 0$. Therefore, when the system presents strong correlations within the disorder distribution, the localization length of eigenstates within the channel becomes large (in general, of the order of the system size used here). This feature

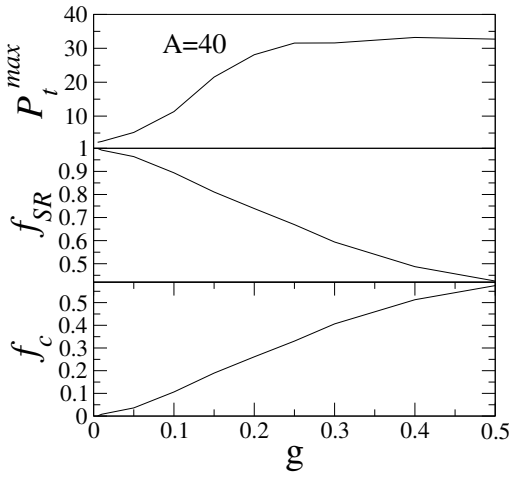

Fig. 9. P_t^{max}, f_{SR} and f_c versus g for $\varepsilon = 0$, $A = 40$, and $L = 60$. For small g, our calculations indicate that the states remain localized between the source and the receiver (in good agreement with the large values of F_{max} and C_{max} obtained previously). For large g the states remain roughly trapped inside the channel and, therefore, the quantum state transference can not take place.

promotes the appearance of QST with good fidelity.

Finally, we exam how the QST depends on the coupling parameters g between the edges S and R and the disordered channel. In figure 8, we take the case with $A = 40$ and evaluate the QST around $\epsilon = 0$. We investigate both C_{max} and F_{max} as a function of g. We noticed that the concurrence and fidelity decrease as we increase the coupling with the channel. We have obtained the same results for $L = 60$ and 120. However, for larger chains, C_{max} and F_{max} become smaller due to the effect of disorder. We can see that the transference of quantum states within this model is almost absent for $g > 0.1$ where both F_{max} and C_{max} decreases considerably. We can build a deeper understanding of this behavior in light of the wave-function topology and its dependence on the value of g. For this analysis, we calculate three functions: the maximum participation number of the time-evolving wave-function; the maximum wave-function on S and R : $f_{SR} = max[|f_1(t)|^2 + |f_{L+2}(t)|^2]$ and the maximum wave-function within the channel: $f_c = max[\sum_{n=2}^{L+1} |f_n(t)|^2]$. All maxima are computed on a long time interval after the initial transient. These three quantities, for $\epsilon = 0$, can be found in fig 9. In the absence of coupling, the initial wave-function remains trapped at the sender site, as expected. We observe that the maximum participation number increases as we increase the value of g. In the small g regime, the wave-function remains more compact. It just slowly leaks towards the channel, eventually focusing at the Receiver. This reasoning is consistent with the large value of f_{SR} and small value of f_c. For stronger couplings, the leaking from the Sender towards the channel is faster and the wave-function spreads over the chain before reaching the receiver. Due to the random nature of the potential, the wave-function looses its coherence and no efficient transfer to the Receiver can be

realized. Maximum value of f_{SR} is smaller than unit, which means that the initial state is never recovered on a long-time run.

4. Conclusions

In summary, we studied the transference of quantum states from a source S to a receiver R connected by a channel with correlated disorder. The correlated disorder inside the channel was constructed here based on a characteristic effective correlation length A. We showed that the localization length of the channel eigenstates, quantified by the participation function, presents a universal finite-size scaling behavior when the system size is measured in units of the disorder correlation length. The eigenstates around the band center are localized over a finite segment of the channel for $L >> A$ while they become effectively extended for $L << A$, thus opening the possibility of the quantum state transfer from the Sender to the Receiver mediated by such disordered channel. We showed that, in the regime of $L << A$, an efficient QST process can take place when the coupling of the Sender and Receiver sites with the channel is weak. This favors a slow leaking from the Sender to the channel, which possibilities the wave-function to reach the Receiver before loosing the coherence with the initial Sender state. For strong couplings, the state at the Sender is fastly transferred to the channel and, due to the random character of the on-site energies, looses coherence before reaching the channel which impairs the QST process. The present results support the general picture that a proper engineering of the on-site potentials and coupling along a disordered channel has to be considered to reach an efficient quantum state transfer for quantum communication protocols.

5. Acknowledgments

This work was partially supported by CNPq, CAPES, and FINEP (Federal Brazilian Agencies), as well as FAPEAL (Alagoas State Agency).

References

1. Y.-T. Huang, J.-D. Lin, H.-Y. Ku, Y.-N. Chen, Phys. Rev. Res. 3 (2021) 023038.
2. J. Xu, T. Liu, Results in Physics 44 (2023) 106157.
3. Y. Chen, L. Zhang, Y. Gu, Z.-M. Wang, Phys. Lett. A 382 (39) (2018) 2795–2798.
4. M. Amazioug, B. Maroufi, M. Daoud, Phys. Lett. A 384 (27) (2020) 126705.
5. N. B. Dehaghani, F. L. Pereira, IFAC-PapersOnLine 55 (16) (2022) 214–219, 18th IFAC Workshop on Control Applications of Optimization CAO 2022.
6. P. Serra, A. Ferrón, O. Osenda, Phys. Lett. A 449 (2022) 128362.
7. A. Saha, A. K. Sarma, Phys. Lett. A 393 (2021) 127176.
8. D. Acosta Coden, S. Gómez, A. Ferrón, O. Osenda, Phys. Lett. A 387 (2021) 127009.
9. E. Fel'dman, A. Pechen, A. Zenchuk, Phys. Lett. A 413 (2021) 127605.
10. S. Bose, Phys. Rev. Lett. 91 (20) (2003) 207901.
11. Y. Matsuzaki, V. M. Bastidas, Y. Takeuchi, W. J. Munro, S. Saito, J. of the Phys. Soc. of Japan 89 (4) (2020) 044003.

12. S. Hermes, T. J. Apollaro, S. Paganelli, T. Macrì, Phys. Rev. A 101 (5) (2020) 053607.
13. G. Gualdi, V. Kostak, I. Marzoli, P. Tombesi, Phys. Rev. A 78 (2) (2008) 022325.
14. D. Wanisch, S. Fritzsche, Phys. Rev. A 102 (3) (2020) 032624.
15. A. Kay, International Journal of Quantum Information 8 (04) (2010) 641–676.
16. S. Lorenzo, T. J. Apollaro, A. Trombettoni, S. Paganelli, International Journal of Quantum Information 15 (05) (2017) 1750037.
17. F. M. D'Angelis, F. A. Pinheiro, D. Guéry-Odelin, S. Longhi, F. Impens, Phys. Rev. Research 2 (3) (2020) 033475.
18. G. M. Almeida, F.A.B.F. de Moura, T. J. Apollaro, M. L. Lyra, Phys. Rev. A 96 (3) (2017) 032315.
19. G. M. Almeida, F.A.B.F. de Moura , M. L. Lyra, Phys. Lett. A 382 (20) (2018) 1335–1340.
20. G. M. Almeida, M. L. Lyra, F.A.B.F. de Moura, Quantum Inf. Processing 18 (11) (2019) 350.
21. A. Zwick, G. A. Álvarez, J. Stolze, O. Osenda, Phys. Rev. A 85 (2012) 012318.
22. L. D. da Silva, A. Ranciaro Neto, M.O. Sales, J.L.L. dos Santos, F. A. B. F. de Moura, Annals of the Brazilian Academy of Sciences 91(2) (2019) e20180114.
23. L. S. Soares, R. D. dos Santos, F. J. S. Sousa, M. O. Sales, F. A. B. F. Moura, International Journal of Modern Physics C 31 (12) (2020) 2050176.
24. R. F. Dutra, M. S. S. Junior, D. Messias, C. V. C. Mendes, M. O. Sales, F. A. B. F. de Moura, International Journal of Modern Physics C (2023). doi:10.1142/S0129183123501103, [link].
URL https://doi.org/10.1142/S0129183123501103
25. B. Kramer, A. MacKinnon, Reports on Progress in Physics 56 (12) (1993) 1469.
26. F. A. B. F. de Moura, International Journal of Modern Physics C 22 (1) (2011) 63–69.
27. W. K. Wootters, Phys. Rev. Lett. 80 (1998) 2245–2248.
28. [link].
URL https://www.netlib.org/lapack/
29. T. J. Apollaro, G. M. Almeida, S. Lorenzo, A. Ferraro, S. Paganelli, Phys. Rev. A 100 (5) (2019) 052308.
30. F.-H. Ren, Z.-M. Wang, Y.-J. Gu, Quantum Inf. Processing 18 (6) (2019) 1–11.